Limnol. Oceanogr., 44(5), 1999, 1304–1315

Oxic/anoxic oscillations and organic carbon mineralization in an estuarine maximum turbidity zone (The Gironde, France)

Gwenaël Abril[1] *and Henri Etcheber*
Université Bordeaux I, Département de Géologie et Océanographie, DGO-UMR 5805, Avenue des Facultés, F-33405 Talence, France

Pierre Le Hir and Philippe Bassoullet
Institut Français de Recherche et d'Exploitation de la Mer, Centre de Brest, BP 70, F-29280 Plouzané, France

Bernard Boutier
Institut Français de Recherche et d'Exploitation de la Mer, Centre de Nantes, BP 21105, F-44311 Nantes, France

Michel Frankignoulle
Université de Liège, Mécanique des Fluides Géophysiques, Unité d'Océanographie Chimique, Institut de Physique (B5), B-4000 Sart Tilman, Belgium

Abstract

The study of vertical particle dynamics in the highly turbid Gironde Estuary has shown intense cycles of sedimentation and resuspension at both diurnal and neap-spring time scales. Fluid mud, with suspended particulate matter (SPM) concentrations between 50 and 500 g liter^{-1}, has been observed during neap tides. Vertical profiles of biogeochemical parameters have been measured in the fluid mud. Anoxic conditions have been detected when SPM concentration exceeded 50 g liter^{-1} in the upstream and 140 g liter^{-1} in the downstream parts of the maximum turbidity zone (MTZ). At the downstream part of the MTZ, anoxic fluid mud was partitioned into a denitrification layer (SPM = 140–250 g liter^{-1}), intensively reworked at the tidal time scale, and by an Mn(IV)-reduction layer (SPM $>$ 250 g liter^{-1}) preferentially reworked at the neap-spring time scale. Due to the alternation of sedimentation and resuspension periods, most of the sediment experienced oxic/anoxic oscillations throughout the neap-spring cycle. Fluid mud resuspension occurred without any observable incidence on the surface-water oxygenation. An increase in total alkalinity was found in the fluid mud, due to both anaerobic respiration and a carbonate dissolution coupled to aerobic respiratory CO_2 generation. This phenomenon significantly affected the inorganic carbon budget of the estuary, increasing the HCO_3^- input to the coastal ocean and reducing the CO_2 flux to the atmosphere. An accumulation of labile-dissolved organic carbon observed in the fluid mud suggests that these oscillations result in an acceleration of particulate organic matter (POM) decomposition. In the Gironde MTZ, a net loss of refractory land-derived POM occurs. This system acts as an efficient oxic/suboxic ''fluidized bed reactor,'' similar to mobile deltaic muds.

Understanding processes affecting carbon distribution through estuaries is of major importance for a better assessment of the contribution of world rivers to the carbon budget of the coastal ocean. The influence of tides in macrotidal estuaries increases the residence times of both water and suspended matter. This forms MTZs, where photosynthesis is strongly limited by light availability (Cole et al. 1992; Fishez et al. 1992; Irigoien and Castel 1997) and where allochthonous materials originating from soil erosion and river-borne phytoplankton detritus are predominant (Relexans et al. 1988; Small et al. 1990; Bianchi et al. 1993). Heterotrophic activity, enhanced by high turbidity (Crump et al. 1998), results in a net mineralization of a major part of the particulate organic carbon (POC) (Wollast 1983; Smith and Hollibaugh 1993; Keil et al. 1996; Gattuso et al. 1998), producing CO_2 that interacts with the carbonate system (Kempe

[1] Present address: Université de Liège, Mécanique des Fluides Géophysiques, Unité d'Océanographie Chimique, Institut de Physique (B5), B-4000 Sart Tilman, Belgium.

Acknowledgments

This work has been funded by the European Commission in the framework of the Biogest project (ENV4-CT96-0213); this is a contribution of the Eloise Projects network. It was also supported by the URM 13 project, linking IFREMER and the University of Bordeaux I.-DGO-UMR 5805. Fieldwork was carried out onboard the RV *Gwen Drez* (IFREMER, France), the RVs *Côte d'Aquitaine* and *Côte de la Manche* (INSU, France), and the RV *Belgica* (Belgium); we thank captains and crews. A. De Resseguier (DGO) built the fluid mud sampler and was present on the field for sampling assistance. We are grateful to P. Castaing and A. Sottolichio (DGO) for help in using the OBS and to A. V. Borges (University of Liège) and E. Lemaire (DGO) for analytical help. We thank N. Iversen (University of Aalborg, Denmark) for helpful discussion in the field and J. Middelburg (NIOO, The Netherlands) for comments on early versions of the manuscript. S. Riou and R. De Wit (DGO) also provided comments on the nitrogen data. Comments of two anonymous reviewers considerably improved the quality of the final version of the manuscript. G.A. was funded by an Environment and Climate EC doctoral grant (ENV4-CT96-5034). M.F. is a research associate of the FNRS (Belgium).

1982) and is released to the atmosphere (Frankignoulle et al. 1998). Dissolved organic carbon (DOC) generally exhibits a conservative behavior in estuaries (Mantoura and Woodward 1983; Prahl and Coble 1994), but significant positive deviations from conservative mixing have been found, for instance, in Chinese turbid estuaries, in relation with sediment resuspension (Cauwet and Mackenzie 1993).

Indeed, in the MTZ, exchange of particles between water and surface sediments is intense and mainly controlled by the tidal regime. Two superimposed cycles of sedimentation and resuspension coexist: neap tides are sedimentation periods, whereas spring tides are dominated by erosion (15-d lunar cycle). Moreover, high- and low-water slacks are sedimentation periods, whereas midebb and midflood are erosion periods (semidiurnal cycle) (Inglis and Allen 1957; Allen et al. 1980; Le Hir and Karlikow 1991; Parker et al. 1994; Reed and Donovan 1994; Grabemann et al. 1997). During neap-tide minimum energy periods, surface turbidities are considerably lower, and hyperconcentrated benthic layers (named ''fluid mud'' by Inglis and Allen 1957) accumulate on the bottom. With increasing tidal amplitudes, a major part of this deposited material is resuspended, and only the most compacted part is definitely sedimented and lost for the system at a fortnightly scale (Allen et al. 1980). Changes also occur at a seasonal scale in relation with river flow variations, and, for instance, a fluid mud deposited upstream during low river discharge can be swept out during flood events.

The presence of an oxygen minimum, corresponding to estuarine MTZ (Morris et al. 1982), and the anoxic status of fluid mud (Sylvester and Ware 1976) have been known for a long time. Recent works have shown that oxygen concentrations in surface water can be considerably lower a few days after neap tide, during resuspension (Parker et al. 1994; Thouvenin et al. 1994). It is thus obvious that particulate material is submitted to oxic conditions during spring tides and to anoxic conditions in fluid mud during neap tides. Surprisingly, very few biogeochemical studies describe the behavior of carbon, nitrogen (Maurice 1994), trace metals (Donard 1983; Morris et al. 1986), or any other element or contaminant that might be affected by these oxic/anoxic oscillations.

This paper is based on data collected in the MTZ of the Gironde Estuary. Its aim is to describe the vertical particle dynamics during a neap-spring tide cycle and the resulting oxygen distribution, to identify the major anoxic processes in the fluid mud, and to observe the response of organic and inorganic carbon to these changing conditions. Furthermore, we evaluate the relative importance of anoxia and discuss the impact of oxic/anoxic oscillations on the organic and inorganic carbon dynamics in the estuary.

Methods

Study area—The Gironde Estuary (Fig. 1), SW France, formed by the junction of the Garonne and Dordogne Rivers, has an average annual freshwater discharge value of around 1,000 $m^3\ s^{-1}$, with a maximum (1,800 $m^3\ s^{-1}$) in February and a minimum (400 $m^3\ s^{-1}$) in August–September. The tidal

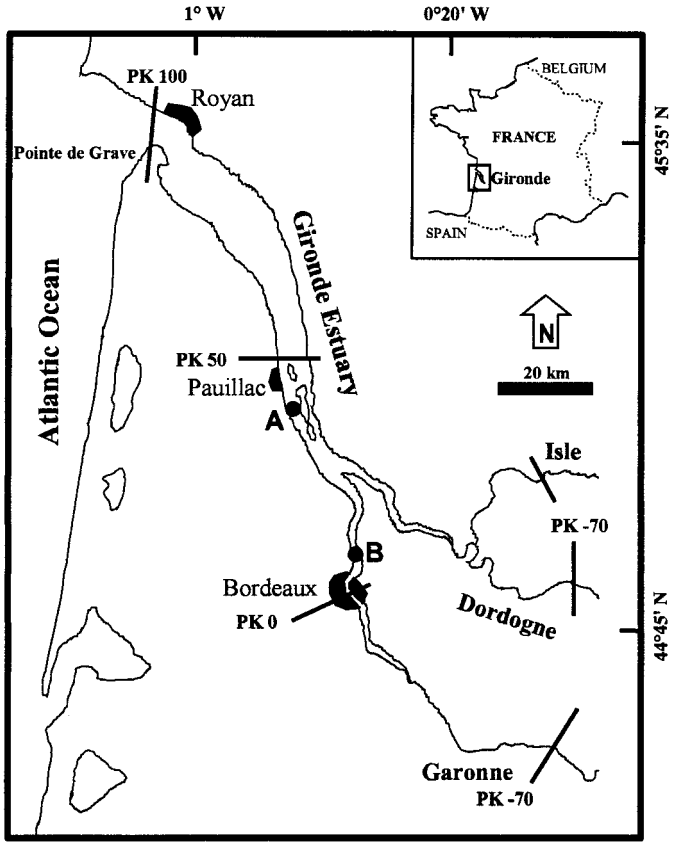

Fig. 1. Map of the Gironde Estuary showing the fluid mud sampling Sta. A, B. PK = distance expressed in kilometers from the city of Bordeaux.

amplitude at the mouth (PK 100) varies from 1.6 m at neap tides to 5 m at spring tides (Allen 1972). Residence time of water in the estuary ranges from 20 to 86 d depending on the season (Jouanneau and Latouche 1981). The upstream limit of the saline intrusion is located around Bordeaux (PK 0) during low river discharge and PK 70 during high river discharge. In the zone of convergence of residual currents, a well-developed turbidity maximum is formed, with SPM concentrations >1 g $liter^{-1}$ at the surface. The supply of particles by riverine transport into this MTZ is continuous throughout the year. On the contrary, most of the exportation of particulate material to the adjacent shelf occurs discontinuously as large plumes during exceptional flood events. As a result, a particle entering the Gironde Estuary remains between 1 and 2 yr within the MTZ before being exported to the Atlantic Ocean (Jouanneau and Latouche 1981). This MTZ migrates longitudinally throughout the day, with ebb and flood, and throughout the year, with river flow variations. Vertical particle dynamics within this MTZ is controlled by the tidal amplitude, and during neap tides, fluid mud accumulates on the bottom as distinct pools that may reach 2 m in height, in which SPM concentration exceeds 100 g $liter^{-1}$ (Allen 1972). During lower current periods, up to 70% of the MTZ particles are trapped in the fluid mud at neap tide (Jouanneau and Latouche 1981).

The estuarine particles are mainly composed of clays and silts (Castaing et al. 1984); their POC content is about 1.5% with low seasonal change and is mainly of terrestrial origin (Fontugne and Jouanneau 1987). POC contents vary seasonally only in the riverine and marine parts of the estuary, outside the MTZ, due to phytoplankton contribution (Etcheber 1983). The percentage of labile POM in the MTZ (estimated from proteins, carbohydrates, and lipids) is between 5 and 10% whatever the season, with a small decreasing trend downstream (Lin 1988). As primary production is strongly limited by light availability in the MTZ, chlorophyll *a* (Chl *a*) concentrations are low, in the range of 1–3 μg liter^{-1} (Irigoien and Castel 1997). Organic carbon budget calculations showed that one-half of the POC entering the MTZ is mineralized within the estuary, the rest being exported to the Atlantic Ocean or sedimented in the estuary (Etcheber 1983; Lin 1988). Oxygen concentrations in surface waters are relatively high, compared to other macrotidal turbid estuaries (Morris et al. 1982; Wollast 1983; Parker et al. 1994; Thouvenin et al. 1994), with concentrations close to saturation levels in riverine and marine parts and about 40–60% of saturation in the MTZ (IFREMER 1994, unpubl. data).

Cruises and sampling—Data were obtained during three cruises: June 1996 (Sedigir experiment) and June and September 1997 (Biogest gir 2 and gir 3 cruises). River flows were low, 460 m^3 s^{-1}, 410 m^3 s^{-1}, and 500 m^3 s^{-1}, respectively, allowing the presence of a well-developed MTZ located in the freshwater and the low-salinity region, between PK −30 and 70. Temporal localization of fieldwork and parameters measured are detailed in Table 1.

The Sedigir experiment consisted of following fluid mud deposition and resuspension over time, at an anchor station in the MTZ (PK 43, Sta. A, Fig. 1), during a 14-d neap-spring period. Vertical profiles of turbidity, current velocity, temperature, and density were obtained with the ''SAMPLE'' system described hereafter. Throughout this experiment, 146 profiles were performed, covering 10 tidal periods, with 40–50-min frequency (Table 1). Fluid mud profiles comprised of 2 m were sampled, at Sta. A, at high or low tide slack, with a 20-cm vertical resolution. A sampler was specially designed for this purpose.

In 1997, longitudinal differences were studied; Biogest gir 2 cruise (June 1997) corresponded to a neap tide situation, whereas Biogest gir 3 (September 1997) corresponded to a spring tide situation. In June 1997, fluid mud was sampled in two distinct fluid mud pools in the upstream (PK 12, Sta. B) and the downstream (PK 43, Sta. A) parts of the MTZ. Longitudinal surface-water sampling along the salinity gradient was conducted during 4-d periods for the two cruises. Finally, 100-km longitudinal transects were carried out at the end of each cruise to investigate the water-column oxygenation in two contrasting situations: neap–spring (June 1997) and spring–neap (September 1997). Tidal amplitudes were similar for both transects: 3.7 and 3.4 m, respectively. Transects started at low tide at Pointe de Grave (PK 100) and ended 10 h later at high tide in Bordeaux (PK 0).

Table 1. Temporal location of cruises and sampling over a 15-d neap-spring cycle. S and SS indicate in situ measurement periods for SPM, current speed, and salinity with a 45-min frequency (''SAMPLE'' system) at Sta. A during half a tidal cycle (S) and an entire tidal cycle (SS). A and B indicate fluid mud sampling, respectively, at Sta. A and B; HT or LT, high or low tide; numbers correspond to the height of anoxic fluid mud sampled. On all profiles comprising 2 m, SPM, oxygen, POC, DOC, NO_3^-, NO_2^-, and NH_4^+ were measured. ''Trans,'' 100-km water-column transects conducted during flood: SPM, oxygen, and DOC were measured; ''Sal,'' Biogest surface-water sampling along the salinity gradient: SPM, oxygen, pH, and TAlk were measured.

	Neap tides										Spring tides				
Days	1	2	3	4	5	6	7	8	9	10	11	12	13	14	15
Sedigir		S	SS			SS	SS	SS	SS		SS		SS	SS	S
June 1996		A		A		A	A	A	A*		A*				
		LT		HT		HT	HT	LT	HT		LT				
		0.4		0.0		1.4	0.4	1.2	0.4		0.0				
Biogest gir 2				Sal	Sal	Sal	Sal	Sal		Trans					
June 1997				A,* B†	B, A‡	A,*† B†	B								
				HT, LT	LT, HT	LT, HT	LT								
				2.0, 2.0	0.8, 0.4	0.4, 0.2	1.2								
Biogest gir 3		Trans									Sal	Sal	Sal	Sal	
September 1997															

* Mn^{2+} was measured.
† pH was measured.
‡ pH and TAlk were measured.

In situ measurements—The SAMPLE system (Station Autonome Multiparamètres Programmable pour le Littoral et les Estuaires, Jestin et al. 1994) was deployed during the Sedigir experiment to investigate both the whole-water column and the fluid mud. The system includes a pressure sensor, a magnetometer, a Pt100 temperature sensor, a seven-annular electrode conductivity sensor, a four-electrode spherical electromagnetic current meter, an optical backscatterance sensor (OBS), and an ultrasonic probe to determine the density within the fluid mud. The acquisition system allows a 0.25-s sampling rate. SPM concentrations are obtained after laboratory pre- and postcalibrations using various dilutions of muds from the sampling site.

During the two 100-km transects in 1997, vertical profiles in the water column were obtained with an ISY salinometer, an ISY oxygen meter probe, and an OBS sensor for SPM. Oxygen and SPM calibrations were performed in situ by comparing with results on simultaneous water sampling ($r^2 = 0.982$, $n = 20$ for oxygen; $r^2 = 0.998$, $n = 20$ for SPM).

Chemical analysis—SPM concentrations were determined by drying for very turbid samples (>50 g liter^{-1}) (salt weights were subtracted) and by filtering on Whatman GF/F glass-fiber filters for water samples (<50 g liter^{-1}). Oxygen concentrations were determined in water samples with the standard Winkler method and in fluid mud with a polarographic electrode (KENT), calibrated by Winkler titrations and a fresh sodium dithionate solution for zero. POC was measured on precombusted Whatman GF/F glass-fiber filters in water samples and on centrifuged material (1,500 rpm) in fluid mud samples. A LECO CS-125 analyzer was used, based on direct combustion in an induction furnace and infrared absorption determination of the CO_2 produced. Samples were acidified with HCl 2N to remove carbonates and were dried overnight at 60°C before analysis. Accuracy was ±0.05% of SPM. For DOC and nutrient determinations, water samples were filtered on precombusted Whatman GF/F glass-fiber filters under low vacuum (200 Hg mm), fluid mud samples were centrifuged in precombusted Pyrex vials, and supernatant solutions were filtered on precombusted Whatman GF/F glass-fiber filters. Comparison of the two separation techniques indicated little disruption of particulate material during centrifugation. DOC was measured with a high-temperature catalytic oxidation analyzer (Shimadzu TOC 5000) according to the protocol and blank correction described by Cauwet (1994); replicates showed an accuracy around 0.05 mg liter^{-1}. Ammonium, nitrate, and nitrite were determined by manual colorimetric techniques (Strickland and Parsons 1972) with a precision around 5%.

For dissolved Mn measurements, samples were pushed out of the sampler by nitrogen pressure and recovered in 250-ml centrifuge flasks; after centrifugation (3,500 rpm), the supernatant was filtered on 0.4-μm nucleopore filters and acidified (HNO_3 Suprapur, 1/1000). All of these operations were performed under N_2 atmosphere to avoid oxidation. Dissolved manganese was determined in the acidified filtrate by flameless atomic absorption spectrophotometry after dilution (1/5) in milli-Q water to avoid matrix effect. Highest concentrations were determined by flame atomic absorption spectrophotometry.

pH was measured just after sampling, using a ROSS combination electrode (Orion) calibrated against the National Bureau of Standards (NBS) (Bates 1973). Absolute accuracy was 0.005 NBS units. Total alkalinity (TAlk) was obtained from Gran electrotitration on 100-ml GF/C-filtered samples. Fluid mud was centrifuged before filtration. Reproducibility was 2 μeq kg^{-1}. The partial pressure of CO_2 and the dissolved inorganic carbon (DIC) concentrations were calculated from pH and TAlk with the dissociation constants of carbonic and boric acids, respectively, from Mehrbach et al. (1973) and Lyman (1975) and the CO_2 solubility coefficient from Weiss (1974).

Results

Current velocities in the MTZ and the fluid mud—Recorded velocities at Sta. A displayed a large range of values throughout the neap-spring cycle. At neap tide, the maximum surface current was 1–1.5 m s^{-1} during flood but 1.5–2 m s^{-1} during ebb. At spring tide, the maximum surface currents were similar during both flood and ebb (2 and 2.5 m s^{-1}), but ebb lasted longer.

A rapid downward current decrease was always observed in the fluid mud; for example, during neap tides and maximum flood, current velocities decreased from 1.5 m s^{-1} in the water column to <0.5 m s^{-1} where the SPM concentration reached 50 g liter^{-1}. Within the fluid mud, where the SPM concentration is >200 g liter^{-1}, current was almost zero.

Particle transport throughout tidal and neap-spring cycles—SPM measurements showed a very large range of concentrations (0.1–500 g liter^{-1}). Two classes of fluid mud concentration were remarkably dominant at Sta. A throughout the tidal cycles: a ''liquid mud,'' in the range of 50–70 g liter^{-1}, and a ''soft mud,'' in the range of 250–450 g liter^{-1} (Fig. 2). Between these two classes, steep SPM gradients (''lutoclines,'' Kirby 1988) were observed between 10 and 50 g liter^{-1} and between 70 and 250 g liter^{-1}. These OBS results are confirmed by acoustic densitometer data. At neap tide (Fig. 3), the liquid mud was always present, with a maximum thickness when current was maximum (hours 130 and 137), while a 1-m-thick soft mud layer remained below. At spring tide (Fig. 3), soft mud was not observed, and liquid mud presented a maximum thickness when current was strong (hours 274 and 280). It then disappeared at water slacks (hour 278), due to advection and deposition processes.

Throughout the whole neap-spring period, transport of SPM at Sta. A followed a cycle influenced by the maximum current (Fig. 4). On day 5, the general decrease of current velocities led to the formation of the soft mud. During neap tides (between days 5 and 10), the consolidation process decreased progressively to the height of the soft mud and led to the hard bottom (>400 g liter^{-1}) rise, which was highest just before spring tides (day 10). This consolidated mud was suddenly eroded at spring tide (between days 10 and 11), transformed into liquid mud, and further transported longitudinally with tides.

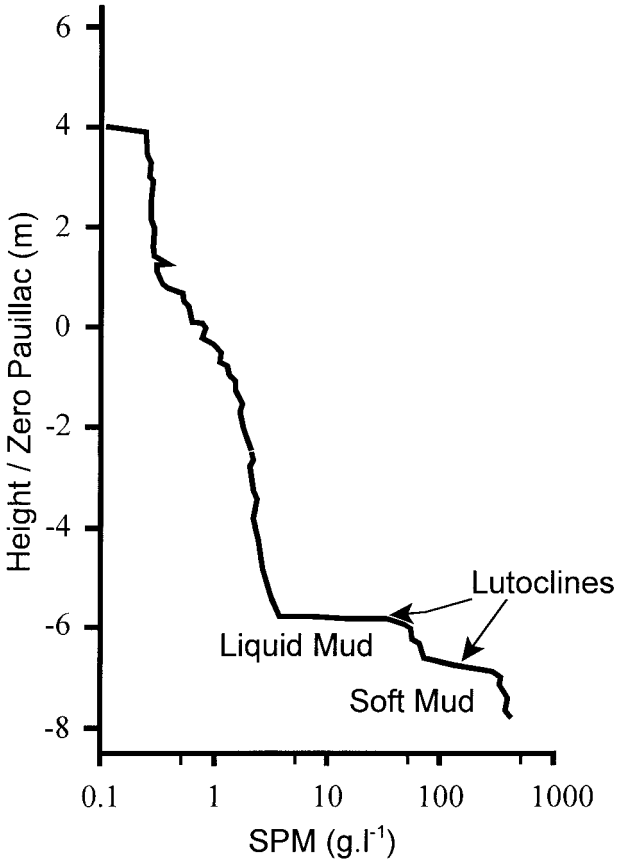

Fig. 2. A typical SPM profile at Sta. A in June 1996 at neap tide, showing the two dominant classes of fluid mud: liquid mud (50–70 g liter^{-1}) and soft mud (250–350 g liter^{-1}). Zero depth corresponds to the mean water level in Pauillac.

Biogeochemical profiles in the fluid mud—Distribution of parameters in bottom water and fluid mud revealed steep vertical gradients. The height of anoxic fluid mud sampled varied between 0.4 and 2 m (Table 1). In 1996, the fluid

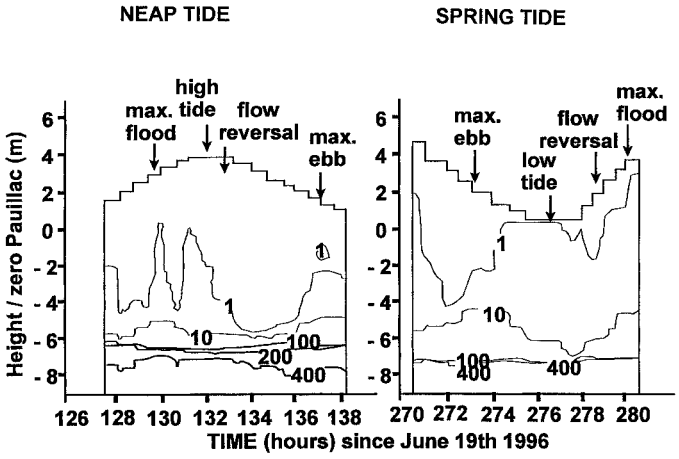

Fig. 3. Distribution of SPM at Sta. A in June 1996, during tidal cycles: neap tide and spring tide. Zero depth corresponds to the mean water level in Pauillac.

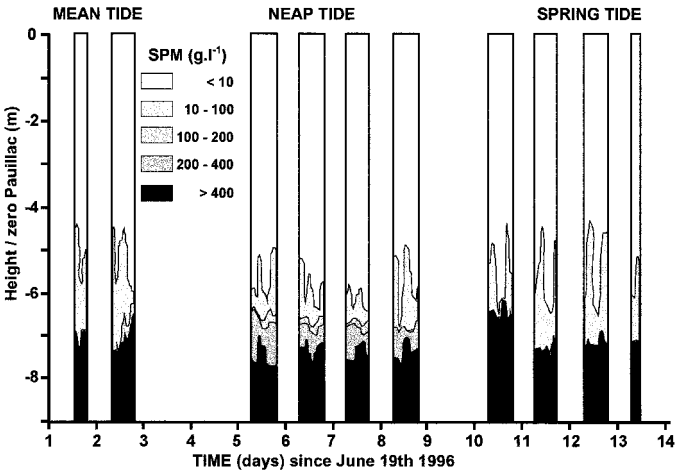

Fig. 4. Distribution of SPM at Sta. A during the studied neap-spring cycle in June 1996. Zero depth corresponds to the mean water level in Pauillac.

mud was more concentrated, and SPM downward increase was considerably higher (400–500 g liter^{-1} m^{-1} at Sta. A) than in June 1997 (120–170 g liter^{-1} m^{-1} at Sta. A and 100–125 g liter^{-1} m^{-1} at Sta. B).

At both stations, the SPM concentration corresponding to the oxic/anoxic interface was constant over time for each station and was equal to 140 g liter^{-1} at Sta. A and to 50 g liter^{-1} at Sta. B (Fig. 5). An in situ oxygen profile performed at Sta. B confirmed these results (Fig. 5).

Two vertical profiles of dissolved constituents at Sta. A are presented in Figs. 6, 7, one including the oxic/anoxic interface (Fig. 6) and one totally anoxic with SPM concentrations reaching 370 g liter^{-1} (Fig. 7). As a general rule, for all profiles, the distributions of these parameters were mainly controlled by the SPM concentrations, and gradients were steeper in compacted fluid mud. The pH drop in the fluid mud was about 0.15 units in 2 m, and most of the decrease occurred around the oxic/anoxic interface. Total alkalinity increased from 2.39 to 2.76 meq kg^{-1} both in the oxic and anoxic levels (Fig. 6). Nitrate concentration decreased to zero in the anoxic fluid mud, indicating denitrification as the major mineralization pathway, when SPM concentrations ranged between 140 and 250 g liter^{-1}. In this layer, a significant increase of nitrite concentrations was observed.

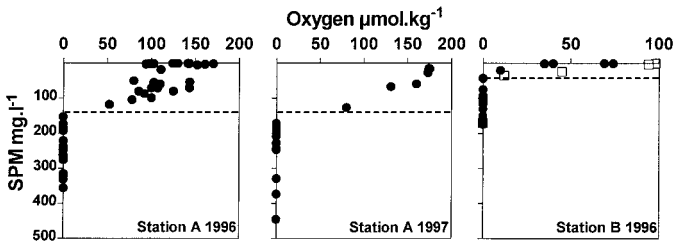

Fig. 5. Oxygen–SPM plot for all bottom water and fluid mud samples at Sta. A in 1996 and 1997 and at Sta. B in 1997 (black circles). White squares are from an in situ profile performed at Sta. B. The oxic/anoxic interface (dotted lines) was constant over time for each station.

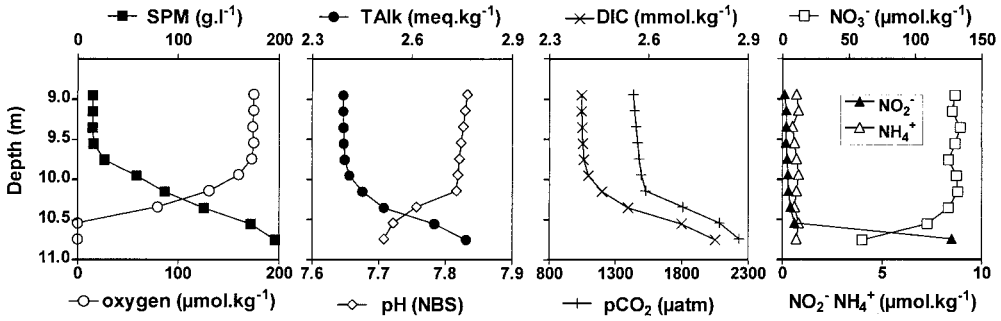

Fig. 6. Vertical distribution of SPM, oxygen, total alkalinity, pH, calculated DIC and pCO_2, NO_3^-, NO_2^-, and NH_4^+ in bottom water and fluid mud. Sta. A, June 1997, neap tide + 1 d, high tide. Zero depth corresponds to the water surface at high-water slack.

When SPM concentrations were >250 g liter^{-1}, Mn^{2+} and NH_4^+ concentrations increased and reached 47 and 15 μmol kg^{-1}, respectively (Fig. 7). Mn(IV) reduction is thus the dominant heterotrophic process in this layer, associated with a strong ammonification. Vertical profiles carried out at Sta. B yielded the following (data not shown): a pH drop was also observed at the oxic/anoxic interface, NO_3^- concentrations also decreased but never reached zero because SPM concentrations were low compared to Sta. A; in the denitrification level, a significant NO_2^- increase was also observed; and NH_4^+ concentrations were constant and were <2 μmol kg^{-1}.

POC vertical distribution showed small but significant oscillations between 1.3 and 1.8% of SPM, without any downward trend (Fig. 8). A net downward increase was found for DOC, with highest concentrations corresponding to anoxic levels. Compared to 2–3 mg liter^{-1} at the surface, concentrations between 2 and 4.5 in bottom oxic waters and up to 6.3 mg liter^{-1} in anoxic fluid mud were measured at Sta. A (Fig. 8a–c). At Sta. B, DOC reached only 4 mg liter^{-1} in the anoxic fluid mud for the earliest profile (Fig. 8d). For the latest profile at Sta. B (neap tide + 3 d), no DOC increase was observed (Fig. 8e). In summary, DOC varied between 2 and 4.5 mg liter^{-1} in the 1–150 g liter^{-1} SPM range at both stations and raised to 5–6.3 mg liter^{-1} in the 150–450 g liter^{-1} SPM range at Sta. A.

Longitudinal surface-water data (4-d cruises)—SPM concentrations in surface water were considerably lower in June

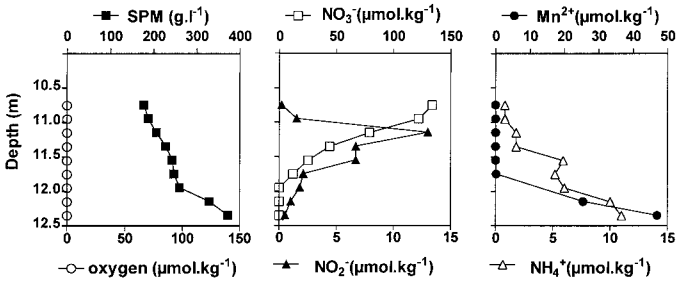

Fig. 7. Vertical distribution of SPM, NO_3^-, NO_2^-, NH_4^+, and Mn^{2+} in a totally anoxic fluid mud profile. Sta. A, June 1997, neap tide, high tide. Zero depth corresponds to the water surface at high-water slack.

(max. = 760 mg liter^{-1}) during neap tide than in September (max. = 1,650 mg liter^{-1}) during spring tide. The distributions of oxygen, pH, and TAlk indicate processes in the low-salinity region (between PK 70 and 30) different from those in the rest of the salinity gradient (Fig. 9). Oxygen decreased from 90% of saturation in the rivers (salinity = 0; PK 70) to 60% in the MTZ (salinity = 0.1; PK 0). Between these two points, pH also showed an important decrease from 7.98 to 7.69 in June 1997 and from 8.22 to 7.75 in September 1997; between salinities 0.1 and 32, oxygen and pH increased in parallel to reach concentrations around the saturation for oxygen and 8.15 for pH. TAlk increased in the low-salinity region and then decreased linearly with estuarine mixing. In September 1997, the TAlk concentration measured in the Dordogne River was considerably lower than in the rest of the estuary.

Water-column transect data—During the two transects performed at mean tides, no fluid mud was observed, and the maximum SPM concentration measured was 50 g liter^{-1}. In June 1997, echosounder observations revealed that most of the fluid mud present 2 d before at Sta. A and B was eroded. In both situations, most of the oxygen variation occurred longitudinally rather than vertically (Fig. 10a). In June 1997, some small decreases in oxygen concentrations with depth, associated with increases in turbidities, were found close to Sta. A, between PK 40 and 70.

DOC concentrations ranged between 1.6 and 3.1 mg liter^{-1} in June 1997 and between 2.1 and 4.2 mg liter^{-1} in September 1997 (Fig. 10b). In both situations, DOC concentrations in the MTZ were significantly higher in bottom samples than in surface ones. Moreover, bottom concentrations were dispersed in the MTZ, whereas surface concentrations showed a linear distribution along the salinity gradient, except at salinities 3 and 5 in September 1997, where concentrations were above the mixing line.

Discussion

Fluid mud dynamics—The Sedigir experiment covered an entire neap-spring cycle (Fig. 4) and gives a complete picture of settling and resuspension processes at Sta. A at both tidal and neap-spring time scales (Table 2). These measurements are representative for a 10–20-km section of the MTZ, where

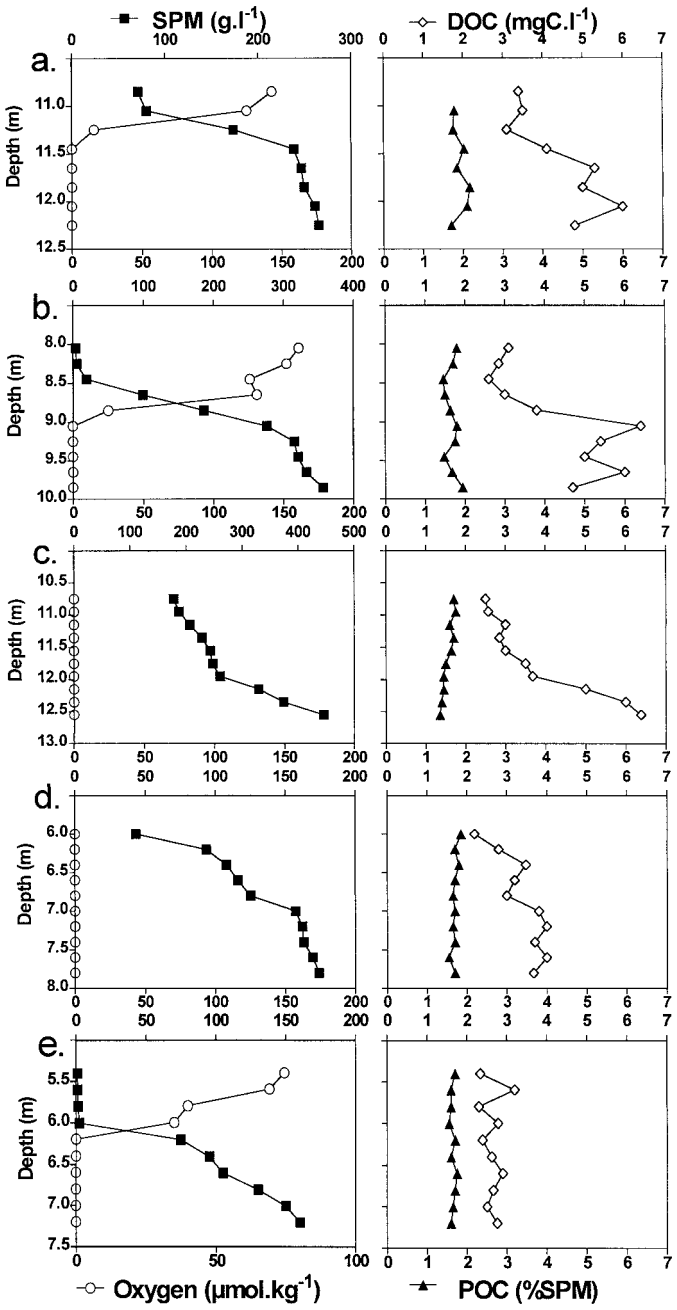

Fig. 8. Vertical distribution of SPM, oxygen, and DOC concentrations and POC content of SPM in bottom water and fluid mud. (a) Sta. A, June 1996, neap tide − 1 d, high tide; (b) Sta. A, June 1996, neap tide + 2 d, low tide; (c) Sta. A, June 1997, neap tide, high tide; (d) Sta. B, June 1997, neap tide − 1 d, low tide; (e) Sta. B, June 1997, neap tide + 3 d, low tide. Zero depth corresponds to the water surface at water slacks.

large fluid mud pools were observed during the experiment. The constitution and progressive consolidation of a thick soft mud layer (ca. 1 m) occurred over 6 d. Its average concentration slowly increased from 250 to 400 g liter^{-1}. The maximum residence time of particles in this nitrate-depleted, Mn^{2+}-rich soft mud was about 6 d.

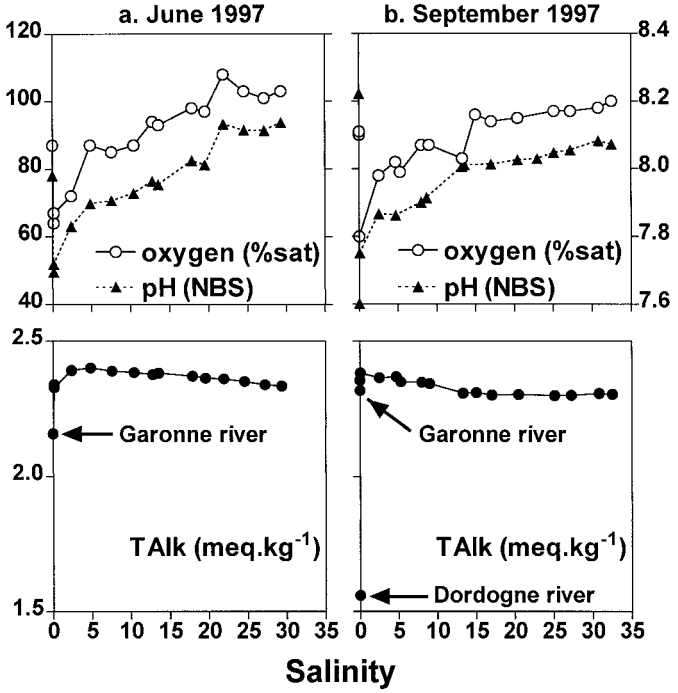

Fig. 9. Distribution of oxygen, pH, and total alkalinity vs. salinity in surface waters; (a) June 1997 neap tide; (b) September 1997 spring tide.

The liquid mud (50–70 g liter^{-1}) is constituted by a partial resuspension of the upper soft mud during neap tides and by the complete resuspension of the consolidate mud at the beginning of spring tides. The rapid decay of velocities within this liquid mud reflects a turbulence damping, which prevents a complete mixing of resuspended materials in the water column. This homogeneous layer exists preferentially during maximum current periods. The residence time of particles in this oxic layer is then rather short (max. = 4 h tidal cycle^{-1}).

Between these liquid mud and soft mud layers, a sharp lutocline is observed; it corresponds to the transition zone from the oxic upper layer to the anoxic soft mud, where denitrification occurs. This layer has a maximum thickness at tide slacks due to deposition processes. Residence time of particles in this zone is also short (max. = 4 h). Exchanges of particles occur preferentially with the upper oxic zone at the tidal time scale, but a fraction of these particles also enters the soft mud pool at each tidal cycle and remains there for several days.

Particles in oxic and anoxic conditions—For each station, the oxic/anoxic interface is situated at a constant SPM concentration: 140 g liter^{-1} at Sta. A and 50 g liter^{-1} at Sta. B (Fig. 5). At Sta. A, this biogeochemical limit corresponds to the second lutocline (70–250 g liter^{-1}), a physically unstable layer (Table 2) where settling and resuspension of particles are intense at the tidal time scale. This supposes that, at these concentrations, the turbulent diffusion of oxygen (that decreases when SPM increases) compensates the biological oxygen demand (that increases when SPM increases). Differ-

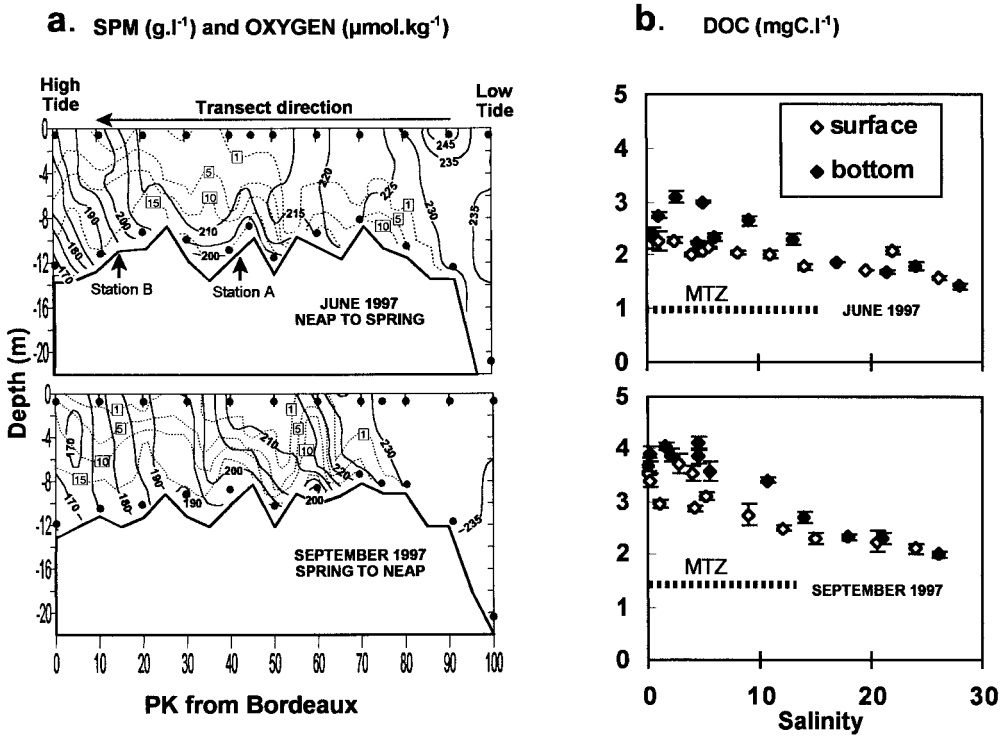

Fig. 10. Transects data. (a) Distribution of SPM (thin dotted lines and enclosed numbers) and oxygen (solid lines) in June and September 1997 in mean tide conditions; black points correspond to water sampling for DOC measurements; reported bottoms correspond to depth obtained by echosounder. (b) Distribution of DOC vs. salinity in surface and bottom waters.

ences in oxygen penetration within the fluid mud between Sta. A and B reflect the downstream decrease in organic matter lability, as reported by Lin (1988). Assuming the SPM concentration of 140 g liter^{-1} is representative for all tidal situations at Sta. A, the percentage of particles in anoxic conditions can be estimated using the SPM profiles

$$\%\mathrm{SPM}_{\mathrm{anox}} = \frac{C_{\mathrm{anox}} \cdot Z_{\mathrm{anox}}}{C_{\mathrm{tot}} \cdot Z_{\mathrm{tot}}}$$

where C_{anox} is the depth-integrated SPM concentration >140 g liter^{-1}, Z_{anox} is the height of fluid mud including concentrations >140 g liter^{-1}, C_{tot} is the integrated SPM concentration of the whole-water column, and Z_{tot} is the water-column height. Two highest SPM limits (450 and 500 g liter^{-1}) were used for the calculation and led to similar results ($\pm$15%): during spring tides, $\%\mathrm{SPM}_{\mathrm{anox}}$ varied between 3% at maximum ebb and 20% at tide slacks; during neap tides, $\%\mathrm{SPM}_{\mathrm{anox}}$ varied between 65% at maximum ebb and flood and 95% at tide slacks. This means that the majority of the particles present around Sta. A experienced one or several oxic/anoxic oscillations throughout the neap-spring cycle. Among the total mass of particles present during neap tides, about one-half remained in the anoxic soft mud for 6 d and was reexposed to oxygen only at the beginning of spring tides. The other half was more frequently reexposed to oxygen during maximum ebb and flood and trapped again in anoxic fluid mud during tide slacks. Results obtained at this station are consistent with the observations of Jouanneau and

Table 2. A summary of fluid mud biogeochemistry at Sta. A.

Layer	SPM (g liter^{-1})	Time scale of sedimentation/erosion	Maximum residence time of particles	Period of maximum thickness	Major processes
Turbid water	0.1–10				Aerobic respiration
First lutocline	10–50				Aerobic respiration
Liquid mud	50–70	Tidal cycle	4 h	Ebb and flood	Aerobic respiration and carbonate dissolution
Second lutocline		Tidal cycle	4 h	Tide slacks	
	70–140				Aerobic respiration and carbonate dissolution
	140–250				Denitrification
Soft mud	250–500	Neap-spring cycle	6 d	Neap tides	Mn reduction

Table 3. Stoichiometric analysis of data from the six deepest levels presented in Fig. 7. Δ is the difference between the two following depths: level 1, between 9.75 and 9.95 m and level 5, between 10.55 and 10.75. All concentrations expressed in μmol kg^{-1}, except TAlk in μeq kg^{-1}. In oxic conditions, ΔHCO_3^- from Corg is equal to ½ ΔTAlk according to the carbonate dissolution reaction; ΔCO_2 from Corg is ΔDIC − ΔTAlk, assuming that all the CO_2 produced from respiration is not involved in the dissolution reaction, a fraction remaining as dissolved CO_2. Expected oxygen consumption includes a respiration term and a nitrification term estimated using the C/N molar ratio (Middelburg unpubl. data). Expected and measured ΔO_2 are in agreement. At the interface, part of ΔTAlk and ΔCO_2 is first attributed to denitrification and equal to ΔNO_3^- and ¼ ΔNO_3^-, respectively; the remaining ΔTAlk and ΔCO_2 are attributed to carbonate dissolution. In anoxic conditions, the observed ΔTAlk is two times higher than the measured ΔNO_3^-.

	Level	ΔTAlk	ΔDIC	ΔHCO_3^- from Corg	ΔCO_2 from Corg	Expected ΔO_2	Measured ΔO_2	Measured ΔNO_3^-
Oxic. Aerobic respiration and carbonate dissolution ($CaCO_3 + CH_2O + O_2 \rightarrow Ca^{2+} + 2HCO_3^-$)								
	1	+14	+15	+7	+1	−9	−13	
	2	+40	+48	+20	+8	−30	−29	
	3	+64	+79	+32	+15	−52	−51	
Interface								
	4	+152	+164					
Aerobic respiration and carbonate dissolution				+68	+8	−84	−80	
Denitrification								
($5CH_2O + 4NO_3^- \rightarrow 4HCO_3^- + CO_2 + 3H_2O + 2N_2$)				+16	+4			−16
Anoxic. Denitrification								
	5	+95	+101	+95	+6			−49

Latouche (1981), who estimated that, during neap tides, up to 70% of the particles of the whole-estuarine MTZ are trapped in the fluid mud.

At Sta. B, we did not perform high-frequency SPM measurements. However, several facts suggest that oxic/anoxic oscillations are also important and that they occur with an even higher frequency: the total mass of particles is two–three times higher, and water-column oxygen concentrations are lower (Fig. 10a); the fluid mud becomes anoxic faster (Fig. 5); and current speeds are higher in this narrow and shallow part of the estuary, particularly during maximum flood: 2.5 m s^{-1} at spring tide compared to 2 m s^{-1} at Sta. A (Allen 1972).

Water-column oxygenation—In estuarine MTZ, oxygen distribution results from surface reaeration and biological and chemical consumption. Oxygen consumption can be classified into three components: (1) water-column respiration, which increases with SPM concentrations; (2) sediment respiration; and (3) resuspension processes, which include a dilution term due to the input of anoxic pore water and a consumption term due to the oxidation of organic and inorganic species produced in the fluid mud (e.g., DOC, NH_4^+, and Mn^{2+}). In other macrotidal estuaries (Loire and Severn Estuaries, Parker et al. 1994; Thouvenin et al. 1994), the latter component is important because oxygen deficits in surface waters were reported during several days after resuspension events. This is not the case in the Gironde MTZ, where reaeration is sufficient to maintain relatively high oxygen concentrations in the MTZ after resuspensions (Fig. 10a). Several reasons might explain this difference from one estuary to the other: (1) differences in the percentage of the volume of water trapped in the fluid mud, depending on the total mass of the MTZ and hydrological conditions; or (2) differences in POC content and in the lability of organic matter. In the Gironde MTZ, the POC content is only 1.5%, and the lability of POM is <10% (Lin 1988). The anaerobic production in the fluid mud of reduced species that consume oxygen during resuspensions is consequently lower than in the Loire Estuary, for instance, where POC contents are around 4% (Maurice 1994).

Stoichiometry of early diagenesis and carbonate dissolution in the fluid mud—The stoichiometry of organic matter decomposition in marine sediments has been fully described by Froelich et al. (1979). Our data show that in the fluid mud, oxygen, nitrate, and manganese (IV) reductions follow each other in succession (Table 2). The Fe(III) reduction presumably also occurs in the most compacted levels of the fluid mud, close to the interface with the hard bottom. We did not detect any sulfide in the fluid mud (Abril unpubl. data), so that neither sulfate reduction nor methanogenesis apparently occurs in the fluid mud. An analysis of the profile presented in Fig. 7, dominated by aerobic processes and denitrification, is given in Table 3.

In oxic conditions, respiration acidifies the system by producing CO_2 and does not significantly affect the TAlk, except if carbonate dissolution occurs. Indeed, the increase in TAlk observed in the fluid mud at Sta. A (Fig. 7) starts above the oxic/anoxic interface at an SPM concentration of 50 g liter^{-1} (Table 2). A dissolution simply related to undersaturation with carbonate mineral would lead to an increase in TAlk twice that of the DIC. This is not the case here because the increases of TAlk and DIC are close to each other; this dissolution is due to the input of CO_2 generated by aerobic respiration (Moulin et al. 1985; Jahnke et al. 1997; *see reaction in Table 3*). According to this stoichiometry, the inorganic carbon increase and the oxygen decrease are in a good agreement (Table 3).

In anoxic conditions, denitrification acidifies the system

Table 4. Inorganic carbon budget of the Gironde Estuary in September 1997.

	tC d^{-1}
HCO_3^- production in the MTZ*	180
HCO_3^- output to the sea†	1,234
CO_2 transfer to the atmosphere‡	380

* TAlk increase of 0.32 meq kg^{-1} and river flow of 500 m^3 s^{-1}.
† Linear extrapolation of TAlk to salinity zero 2.38 meq kg^{-1} and river flow.
‡ Direct air–sea flux measurement (Frankignoulle et al. 1998).

by producing CO_2 but also increases the TAlk by producing HCO_3^-. However, the observed increase in TAlk is two times higher than what it should be from denitrification. One probable explanation is that biogeochemical profiles sampled at water slack are not at steady state, as reported by Aller et al. (1996) in Amazon shelf mud. Indeed, particle deposition might go faster than homogenization of dissolved species by turbulent diffusion. When settling, particles trap pore water with chemical properties resulting from previous processes. In our case, part of the high TAlk observed is probably due to an earlier oxic carbonate dissolution.

Impact on inorganic carbon budget—The net alkalinity source identified in the MTZ (Fig. 9) significantly affects the carbon budget of the estuary (Table 4). In September 1997, taking into account the contribution of the two rivers, the TAlk increase in the MTZ was equal to 0.32 meq kg^{-1} and corresponded to 14% of the total HCO_3^- output to the coastal ocean. This HCO_3^- is produced by anaerobic organic carbon decomposition and $CaCO_3$ dissolution, which both reduce the CO_2 production in the estuary. In the case of anaerobic processes, all of the HCO_3^- originates from organic carbon and CO_2, whereas in the case of carbonate dissolution, one-half of the HCO_3^- also originates from carbonate mineral. The reduction of the CO_2 evasion to the atmosphere (Frankignoulle et al. 1998) due to these two processes is thus between 16% (assuming only carbonate dissolution) and 32% (assuming only anaerobic processes).

Implications for organic carbon decomposition—Every year, the Garonne and Dordogne Rivers carry about 93.10^3 tons of POC into the Gironde Estuary (Veyssy 1998): phytoplanktonic-derived material accounts for 15.10^3 tons of POC, i.e., 15% of the total organic load, the rest being a soil-derived material. The labile fractions of these two POM sources (estimated from proteins, carbohydrates, and lipids) are between 75 and 90% in phytoplanktonic material and between 15 and 30% for soil-derived material (Lin 1988). About 50% of the riverine POM entering the estuary is mineralized in this area (Etcheber 1983). Consequently, the Gironde MTZ is an efficient reactor for mineralizing most of the labile POM but also a significant fraction of the refractory soil-derived POM.

This intense mineralization is related to the long residence times of particles in the MTZ (average = 18 months). First, it allows the mixing of labile phytoplanktonic POM, produced in both riverine and marine end members during spring and summer, with the soil-derived refractory POM supplied during fall and winter (Etcheber 1983). This mixing presumably promotes the oxidation of refractory POM by cooxidation and cometabolism (''priming''), as described in marine sediments during bioturbation (Canfield 1994). Secondly, the sediment present in the MTZ experiences up to 36 neap-spring cycles and 100s of tidal cycles before being exported to the shelf. Because fluid mud preferentially exists during low river discharge periods, oxic/anoxic oscillation occurrence has to be relativized according to the season. Anaerobic mineralization, which transforms refractory POM slower than aerobic decomposition (Kristensen et al. 1995), is restricted in time because periodic massive resuspensions occur. In contrast, a DOC accumulation is observed in the anoxic fluid mud (Fig. 8), similar to those reported in anoxic microcosm experiments (Otsuki and Hanya 1972*a,b;* Hansen and Blackburn 1991; Kristensen et al. 1995; Andersen 1996). This DOC supply can be attributed to both desorption processes (Keil et al. 1994), because of surface competition and rapid pH change (Morel et al. 1991), and to the death of aerobic bacteria. Indeed, particle-attached aerobic bacteria are dominant in estuarine MTZ (Zimmermann 1997; Crump et al. 1998) and can be trapped in the anoxic fluid mud, where most of them die after a few days. As a consequence, the growth of anaerobic bacteria is stimulated and could further promote the degradation of refractory POM within the fluid mud. In the same manner, during the ensuing resuspension step, the growth of aerobic bacteria is also stimulated. Figure 10 shows that there is a steep DOC gradient between the bottom and surface waters in the MTZ, which suggests a rapid consumption within the water column. It should be noted that the release of DOC from the sediment can also contribute to this gradient (Burdige and Homstead 1994).

The biogeochemical characteristics of the Gironde MTZ described here are comparable to those reported in deltaic and continental shelf sediments (Alongi 1995; Aller et al. 1996; Aller 1998). Physical reworking of sediments occur on even shorter time scales (tidal and neap-spring; Table 2). Heterotrophic activity is also dominated by bacteria (Canon and Frankignoulle unpubl. thymidine incorporation and bacterial count data) rather than by macro- or meiofauna (Irigoien and Castel 1995); oxic and suboxic processes are dominant; and NH_4^+ and Mn^{2+} produced in the fluid mud are repetitively reoxydized after resuspensions, respectively, by nitrification and precipitation. These characteristics make these systems act as efficient ''fluidized bed reactors'' (Aller 1998) for land-derived refractory POM decomposition.

References

ALLEN, G. P. 1972. Etude des processus sédimentaires dans l'estuaire de la Gironde. Mém. IGBA.

———, J. C. SALOMON, P. BASSOULLET, Y. DU PENHOAT, AND C. DE GRANDPRÉ. 1980. Effects of tides on mixing and suspended sediment transport in macrotidal estuaries. Sediment Geol. **26:** 69–90.

ALLER, R. C. 1998. Mobile deltaic and continental shelf muds as suboxic, fluidized bed reactors. Mar. Chem. **61:** 143–155.

———, N. E. BLAIR, Q. XIA, AND P. D. RUDE. 1996. Remineralization rates, recycling and storage of carbon in Amazon shelf sediments. Cont. Shelf Res. **16:** 753–786.

ALONGI, D. M. 1995. Decomposition and recycling of organic matter in muds of the Gulf of Papua, northern Coral Sea. Cont. Shelf Res. **15:** 1319–1337.

ANDERSEN, F. Ø. 1996. Fate of organic carbon added as diatom cells to oxic and anoxic marine sediment microcosms. Mar. Ecol. Prog. Ser. **134:** 225–233.

BATES, R. G. 1973. Determination of pH. Theory and practice. Wiley.

BIANCHI, T. S., S. FINDLAY, AND R. DAWSON. 1993. Organic matter sources in the water column and sediments of the Hudson River Estuary: The use of plant pigment as tracers. Estuarine Coastal Shelf Sci. **36:** 359–376.

BURDIGE, D. J., AND J. HOMSTEAD. 1994. Fluxes of dissolved organic carbon from Chesapeake Bay sediments. Geochim. Cosmochim. Acta **58:** 3407–3424.

CANFIELD, D. E. 1994. Factors influencing organic carbon preservation in marine sediments. Chem. Geol. **114:** 315–329.

CASTAING, P., J. M. JOUANNEAU, D. PRIEUR, C. RANGEL-DAVALOS, AND L. A. ROMAÑA. 1984. Variations spatio-temporelles de la granulométrie des suspensions de l'estuaire de la Gironde. J. Rech. Océanogr. **9:** 115–119.

CAUWET, G. 1994. HTCO method for dissolved organic carbon analysis in seawater: Influence of catalyst on blank estimation. Mar. Chem. **47:** 55–64.

———, AND F. T. MACKENZIE. 1993. Carbon inputs and distribution in estuaries of turbid rivers: The Yang Tze and Yellow Rivers (China). Mar. Chem. **43:** 235–246.

COLE, J. J., N. F. CARACO, AND B. L. PEIERLS. 1992. Can phytoplankton maintain a positive carbon balance in a turbid, freshwater, tidal estuary? Limnol. Oceanogr. **37:** 1608–1617.

CRUMP, B. C., J. A. BAROSS, AND C. A. SIMENSTAD. 1998. Dominance of particle-attached bacteria in the Columbia River Estuary, USA. Aquat. Microb. Ecol. **14:** 7–18.

DONARD, O. F. X. 1983. Biogéochimie et hydrodynamique d'un système estuarien macrotidal. Ph.D. thesis, Univ. Bordeaux I.

ETCHEBER, H. 1983. Biogéochimie de la matière organique en milieu estuarien: Comportement, bilan, propriétés. Ph.D. thesis, Univ. Bordeaux 1.

FISHEZ, R., T. D. JICKELLS, AND H. M. EDMUNDS. 1992. Algal blooms in high turbidity, a result of the conflicting consequences of turbulence on nutrient cycling in a shallow water estuary. Estuarine Coastal Shelf Sci. **35:** 577–592.

FONTUGNE, M. R., AND J. M. JOUANNEAU. 1987. Modulation of the particulate organic carbon flux to the ocean by a macrotidal estuary: Evidence from measurement of carbon isotopes in organic matter from the Gironde system. Estuarine Coastal Shelf Sci. **24:** 377–387.

FRANKIGNOULLE, M., AND OTHERS. 1998. Carbon dioxide emission from European estuaries. Science **282:** 434–436.

FROELICH, P. N., AND OTHERS. 1979. Early oxidation of organic matter in pelagic sediments of the eastern equatorial Atlantic: Suboxic diagenesis. Geochim. Cosmochim. Acta **43:** 1075–1090.

GATTUSO, J-P., M. FRANKIGNOULLE, AND R. WOLLAST. 1998. Carbon and carbonate metabolism in coastal aquatic ecosystems. Annu. Rev. Ecol. Syst. **29:** 405–434.

GRABEMANN, I., R. J. UNCLES, G. KRAUSS, AND J. A. STEPHENS. 1997. Behaviour of turbidity maxima in the Tamar (U.K.) and Weser (F.R.G.) estuaries. Estuarine Coastal Shelf Sci. **45:** 235–246.

HANSEN, L. S., AND T. H. BLACKBURN. 1991. Aerobic and anaerobic mineralization of organic material in marine sediment microcosm. Mar. Ecol. Prog. Ser. **75:** 283–291.

[IFREMER] INSTITUT FRANÇAIS DE RECHERCHE ET D'EXPLOITATION DE LA MER. 1994. Estuaire de la Gironde, livre blanc. Final report. IFREMER (Brest)—Agence de l'eau Adour Garonne.

INGLIS, C. C., AND F. H. ALLEN. 1957. The Regimen of the Thames Estuary as affected by currents, salinities and river flow. Proc. Inst. Civil Eng. **7:** 827–868.

IRIGOIEN, X., AND J. CASTEL. 1995. Feeding rates and productivity of copepod *Acartia bifilosa* in a highly turbid estuary; the Gironde (SW France). Hydrobiologia **311:** 115–125.

———, AND ———. 1997. Light limitation and distribution of chlorophyll pigments in a highly turbid estuary: The Gironde (SW France). Estuarine Coastal Shelf Sci. **44:** 507–517.

JAHNKE, R. A., D. B. CRAVEN, D. C. MCCORKLE, AND C. E. REIMERS. 1997. $CaCO_3$ dissolution in California margin sediments: The influence of organic matter remineralization. Geochim. Cosmochim. Acta **61:** 2587–3604.

JESTIN, H., P. LE HIR, AND P. BASSOULLET. 1994. The ''SAMPLE'' system, a new concept of benthic station—Oceans '94—Osates Proc. **3:** 278–283.

JOUANNEAU, J. M., AND C. LATOUCHE. 1981. The Gironde Estuary, p. 1–115. *In* H. Fürchtbauer, A. P. Lisitzyn, J. D. Millerman, and E. Seibold [eds.], Contribution to sedimentology **10.** E. Sweizerbart'sche Verlagsbuchhandlung, Stuttgart.

KEIL, R. G., L. M. MAYER, P. D. QUAY, J. E. RICHEY, AND J. I. HEDGES. 1996. Loss of organic matter from riverine particles in deltas. Geochim. Cosmochim. Acta **61:** 1507–1511.

———, D. B. MONTLUÇON, F. G. PRAHL, AND J. I. HEDGES. 1994. Sorptive preservation of labile organic matter in marine sediments. Nature **370:** 549–552.

KEMPE, S. 1982. Valdivia cruise, October 1981: Carbonate equilibria in the estuaries of Elbe, Weser, Ems and in the southern German Bight, p. 719–742. *In* E. T. Degens [ed.], Transport of carbon and minerals in major world rivers. Univ. Hamburg **52.**

KIRBY, R. 1988. High concentration suspension (fluid mud) layers in estuaries, p. 463–487. *In* J. Dronkers and W. Van Leussen [eds.], Physical processes in estuaries. Springer.

KRISTENSEN, E., S. I. AHMED, AND A. H. DEVOL. 1995. Aerobic and anaerobic decomposition of organic matter in marine sediments: Which is faster? Limnol. Oceanogr. **40:** 1430–1437.

LE HIR, P., AND N. KARLIKOW. 1991. Balance between turbidity maximum and fluid mud in the Loire Estuary. Lessons of a first mathematical modelling, p. 449–466. *In* G. Di Silvio, A. Lamberti, and L. Montefusco [eds.], Transport of suspended sediments and its mathematical modelling. IAHR, Univ. Firenze.

LIN, R. G. 1988. Etude du potentiel de dégradation de la matière organique particulaire au passage eau douce -eau salée: Cas de l'estuaire de la Gironde. Ph.D. thesis, Univ. Bordeaux 1.

LYMAN, J. 1975. Buffer mechanism of seawater. Ph.D. thesis, Univ. of California-Los Angeles.

MANTOURA, R. F. C., AND E. M. S. WOODWARD. 1983. Conservative behaviour of riverine dissolved organic carbon in the Serven Estuary: Chemical and geochemical implications. Geochim. Cosmochim. Acta **47:** 1293–1309.

MAURICE, L. 1994. Biodégradabilité de la matière organique dans le bouchon vaseux et la crème de vase de l'estuaire de la Loire. Oceanol. Acta **17:** 501–516.

MEHRBACH, C., C. CULBERSON, J. E. HAWLEY, AND R. M. PYTKOWICH. 1973. Measurements of the apparent dissociation constants of carbonic acid in seawater at atmospheric pressure. Limnol. Oceanogr. **18:** 897–907.

MOREL, F. M. M., D. A. DZOMBAK, AND N. M. PRICE. 1991. Heterogeneous reactions in coastal waters, p. 165–180. *In* R. F. C. Mantoura, J-M. Martin, and R. Wollast [eds.], Ocean margin processes in global change. Wiley.

MORRIS, A. W., A. J. BALES, R. J. M. HOWLAND, G. E. MILLWARD, D. R. ACKROYD, D. H. LORING, AND R. T. T. RANTALA. 1986. Sediment mobility and its contribution to trace metal cycling

and retention in a macrotidal estuary. Water Sci. Technol. **18:** 111–119.

———, D. H. LORING, A. J. BALES, R. J. M. HOWLAND, R. F. C. MANTOURA, AND E. M. S. WOODWARD. 1982. Particle dynamic, particulate carbon and the oxygen minimum in an estuary. Oceanol. Acta **5:** 349–353.

MOULIN, E., A. JORDENS, AND R. WOLLAST. 1985. Influence of the aerobic bacterial respiration on the early dissolution of carbonates in coastal sediments, p. 196–208. *In* R. Wollast and R. Van Grieken [eds.], Progress in Belgium oceanographic research. University of Antwerp, Belgium.

OTSUKI, A., AND T. HANYA. 1972*a*. Production of dissolved organic matter from dead green algal cells. 1. Aerobic microbial decomposition. Limnol. Oceanogr. **17:** 248–257.

———, AND ———. 1972*b*. Production of dissolved organic matter from dead green algal cells. 2. Anaerobic microbial decomposition. Limnol. Oceanogr. **17:** 258–264.

PARKER, W. R., L. D. MARSHALL, AND A. J. PARFITT. 1994. Modulation of dissolved oxygen levels in a hypertidal estuary by sediment resuspension. Neth. J. Aquat. Ecol. **38:** 347–352.

PRAHL, F. G., AND P. G. COBLE. 1994. Inputs and behaviour of dissolved organic carbon in the Columbia River Estuary, p. 451–457. *In* K. R. Dyer and R. J. Orth [eds.], Changes in fluxes in estuaries: Implications from science to management. Academic.

REED, D. J., AND J. DONOVAN. 1994. The character and composition of the Columbia River estuarine turbidity maximum, p. 445–450. *In* K. R. Dyer and R. J. Orth [eds.], Changes in fluxes in estuaries: Implications from science to management. Academic.

RELEXANS, J. C., M. MEYBECK, G. BILLEN, M. BRUGEAILLE, H. ETCHEBER, AND M. SOMVILLE. 1988. Algal and microbial processes involved in particulate organic matter dynamics in the Loire Estuary. Estuarine Coastal Shelf Sci. **27:** 625–644.

SMALL, L. F., C. D. MCINTIRE, K. B. MACDONALD, J. R. LARA-LARA, B. R. FREY, M. C. AMSPOKER, AND T. WENFIELD. 1990. Primary production, plant and detrital biomass, and particle transport in the Columbia River Estuary. Prog. Oceanogr. **25:** 175–210.

SMITH, S. V., AND J. T. HOLLIBAUGH. 1993. Coastal metabolism and the oceanic organic carbon cycle. Rev. Geophys. **31:** 75–89.

STRICKLAND, J. D., AND T. R. PARSONS. 1972. A practical handbook of seawater analysis. Fisheries Research Board of Canada.

SYLVESTER, A. J., AND G. C. WARE. 1976. Anaerobiosis of fluid mud. Nature **264:** 635.

THOUVENIN, B., P. LE HIR, AND L. A. ROMAÑA. 1994. Dissolved oxygen model in the Loire Estuary, p. 169–178. *In* K. R. Dyer and R. J. Orth [eds.], Changes in fluxes in estuaries: Implications from science to management. Academic.

VEYSSY, E. 1998. Transferts de matières organiques des bassins versants aux estuaires de la Gironde et de l'Adour. Ph.D. thesis, Univ. Bordeaux 1.

WEISS, R. F. 1974. Carbon dioxide in water and seawater: The solubility of a non-ideal gas. Mar. Chem. **2:** 203–215.

WOLLAST, R. 1983. Interaction in estuaries and coastal waters, p. 385–407. *In* B. Bolin and R. B. Cook [eds.], The major biogeochemical cycles and their interactions. Wiley.

ZIMMERMANN, H. 1997. The microbial community on aggregates in the Elbe Estuary, Germany. Aquat. Microb. Ecol. **13:** 37–46.

Received: 6 August 1998
Accepted: 15 February 1999
Amended: 19 March 1999